Spin-Peierls transition in the $S = \frac{1}{2}$ compound TiPO$_4$ featuring large intrachain coupling

J. M. Law,[1,2,*] C. Hoch,[1] R. Glaum,[3] I. Heinmaa,[4] R. Stern,[4] J. Kang,[5] C. Lee,[5] M.-H. Whangbo,[5] and R. K. Kremer[1]

[1]*Max Planck Institut für Festkörperforschung, Heisenbergstrasse 1, D-70569 Stuttgart, Germany*
[2]*Physics Department, Loughborough University, Loughborough, Leicestershire, United Kingdom*
[3]*Institut für Anorganische Chemie, Universität Bonn, D-53121 Bonn, Germany*
[4]*National Institute of Chemical Physics and Biophysics, EE-12618 Tallinn, Estonia*
[5]*Department of Chemistry, North Carolina State University, Raleigh, North Carolina 27695-8204, USA*

We investigated the magnetic and structural properties of the quasi-one-dimensional $3d^1$ quantum chain system TiPO$_4$ ($J \sim 965$ K) by magnetic susceptibility, heat capacity, electron spin resonance, x-ray diffraction, and nuclear magnetic resonance (NMR) measurements, and by density functional theory (DFT) calculations. TiPO$_4$ undergoes two magnetostructural phase transitions, one at 111 K and the other at 74 K. Below 74 K, NMR detects two different ^{31}P signals and the magnetic susceptibility vanishes, while DFT calculations evidence a bond alternation of the Ti-Ti distances within each chain. Thus, the 74 K phase transition is a spin-Peierls transition which evolves from an incommensurate phase existing between 111 and 74 K.

The discovery of high-T_c superconductivity in two-dimensional oxocuprates has stimulated broad interest in the properties of low-dimensional quantum $S = 1/2$ antiferromagnets. The complex interplay between spin, charge, orbital, and lattice degrees of freedom in low-dimensional systems with pronounced quantum fluctuation produces a plethora of complex and unusual ground states.[1,2]

Most of the prominent examples of low-dimensional quantum antiferromagnets with exotic ground states contain Cu^{2+} ($3d^9$, $S = 1/2$) ions with one hole present in the e_g orbitals.[3–5] Compounds of early transition-metal elements with one electron in the d shell are less frequently investigated. With a $3d^1$ electron in a high-symmetry or slightly distorted octahedral environment, the orbital degeneracy of the t_{2g} states opens new degrees of freedom, with the possibility of low-energy orbital excitations and the interesting scenario of destabilization of coherent spin or orbital ordering by quantum fluctuations. $3d^1$ systems can be easily realized in compounds containing, e.g., Ti^{3+} or V^{4+} cations. A paramount example is the vanadium ladder compound α'-NaV$_2$O$_5$.[6] At high temperatures α'-NaV$_2$O$_5$ contains mixed-valent vanadium cations with one electron occupying an orbital confined to the rungs of the ladder, hence constituting a quarter-filled ladder system.[7] Below $\sim$34 K α'-NaV$_2$O$_5$ undergoes charge ordering[8] leading to a spin gap of $\sim$100 K indicated by a rapid drop of the magnetic susceptibility. That was initially ascribed to a spin-Peierls transition.[6,9] Other prominent low-dimensional $3d^1$ systems that have recently attracted much attention are the Mott insulators TiOX ($X =$ Cl, Br).[10–14] These compounds crystallize in the FeOCl-type structure, consisting of Ti-O-X layers made up of TiO$_4$Cl$_2$ octahedra. These layers are stacked, with van der Waals interactions between them.[15,16] The magnetic susceptibility of TiOCl reveals several unusual features, which led to the proposal that TiOCl may be a manifestation of a resonating-valence-bond solid.[10] Subsequently, Seidel *et al.* demonstrated that the high-temperature susceptibility fits very well to an $S = 1/2$ Heisenberg chain model with nearest-neighbor (NN) antiferromagnetic (AFM) spin-exchange (SE) interaction of $\sim$660 K. In view of these

findings and their local density approximation $+ U$ electronic structure calculations, Seidel *et al.* concluded that TiOCl is an example of a Heisenberg chain that undergoes a spin-Peierls transition at 67 K.[11] Subsequent low-temperature x-ray structure determination showed a slight dimerization of the Ti-Ti distances along the b direction.[17] A further anomaly was detected at $T_{c2} = 95$ K, which signals a transition into an incommensurate phase with a slight monoclinic distortion of the lattice. It was initially believed and it appears to be now generally accepted to be of continuous or higher order; however, there was a later claim that it was first order.[14,18–21]

Here, we report the magnetic and structural properties of TiPO$_4$, which contains Ti^{3+} cations and displays two magnetostructural phase transitions reminiscent of those in TiOX. In contrast to TiOCl, however, TiPO$_4$ is a structurally one-dimensional compound crystallizing in the CrVO$_4$ structure type (space group $Cmcm$) (see inset in Fig. 1).[22] The Ti^{3+} ions, carrying $S = 1/2$ entities, are subject to axially compressed TiO$_6$ octahedra. These share their edges to form corrugated TiO$_4$ ribbon chains along the c axis with a buckling angle of $156.927(4)^{\circ}$ in the a-c plane. The Ti^{3+}-Ti^{3+} distance at room temperature (RT) amounts to $3.1745(10)$ Å with a Ti^{3+}-O^{2-}-Ti^{3+} $\angle$ of $95.484(5)^{\circ}$.[23] The TiO$_4$ ribbon chains are interconnected by sharing corners with distorted PO$_4$ tetrahedra.

At high temperature the magnetic susceptibility of a polycrystalline sample (Fig. 1, main panel) is characterized by a broad maximum centered at $\sim$625 K, indicating short-range AFM correlations. After correction for a temperature-independent offset to the susceptibility arising from diamagnetic contributions of the closed shells and van Vleck terms, the high-temperature magnetic susceptibility can be described very well by an $S = 1/2$ Heisenberg chain with a uniform NN AFM SE interaction[24] of 965(10) K and a g factor of 1.94(3).

Below $\sim$120 K the susceptibility reveals two subsequent magnetic phase transitions, indicated by two rapid drops of the susceptibility at 111(1) and 74(0.5) K. Finally, at the lowest temperatures the susceptibility levels off to a value of $75(10) \times 10^{-6}$ cm^3/mol. At very low temperature a slight
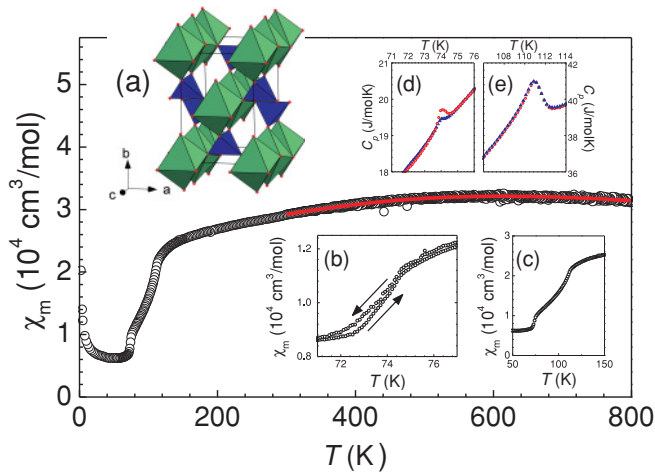
FIG. 1. (Color online) (o) Molar magnetic susceptibility χ_m of $TiPO_4$ measured in a field of 1 T. The (red) line is a fit to a Heisenberg chain with uniform NN AFM SE interaction; see text. Insets: (a) Crystal structure of $TiPO_4$, where large green and small blue polyhedra represent the TiO_6 octahedra and PO_4 tetrahedra, respectively. (b),(c) χ_m in the region of the phase transitions. (d),(e) Heat capacity C_p in the region of the anomalies, where the red circles and blue triangles refer to the heating and cooling data, respectively.

increase is seen, which we ascribe to a Curie tail due to $\sim$70 ppm of free $S = 1/2$ spin entities. The anomaly at 74 K shows a thermal hysteresis with a temperature difference of $\sim$50 mK between the heating and cooling traces while heating/cooling cycles gave identical susceptibilities for the 111 K anomaly [see Fig. 1 insets (b),(c)].

Heat capacities collected on crystals exhibit two λ-type anomalies at 110.9(0.6) and 74.1(0.3) K, with the lower-temperature anomaly also showing a thermal hysteresis, while again no hysteresis is seen for the higher-temperature anomaly [see Fig. 1 insets (d),(e)]. Angular- and temperature-dependent electron spin resonance (ESR) measurements on single crystals revealed a single Lorentzian resonance line (g factor 1.93–1.95) and a linewidth decreasing linearly with temperature (50 $\leqslant$ full width at half maximum $\leqslant$ 300 Oe) consistent with earlier findings.[22,25] The integrated intensity of the ESR line mimics the temperature dependence of the magnetic susceptibility and drops to zero below 74 K.

The crystal structure of a very high-quality single crystal of $TiPO_4$ was determined by x-ray single-crystal diffraction measurements at various temperatures between 293 and 90 K. Down to 90 K the structure was found to be identical to that reported by Glaum and Gruehn, except for small changes of the lattice parameters and the general atomic positions.[23] As the temperature is lowered from RT to $\sim$120 K, the lattice parameters a and b increase slightly but the c parameter decreases, such that the cell volume remains almost constant. The residual electron density, i.e., the measured electron density minus the calculated electron density (from the superposition of spherical atom densities), shows considerable residuals located within the a-c plane next to the Ti atoms, at an interstitial position in the ribbon chain, and at a position bisecting the O-Ti-O angle perpendicular to the ribbon chains. Upon cooling there is a gradual migration of the density away from the bisecting
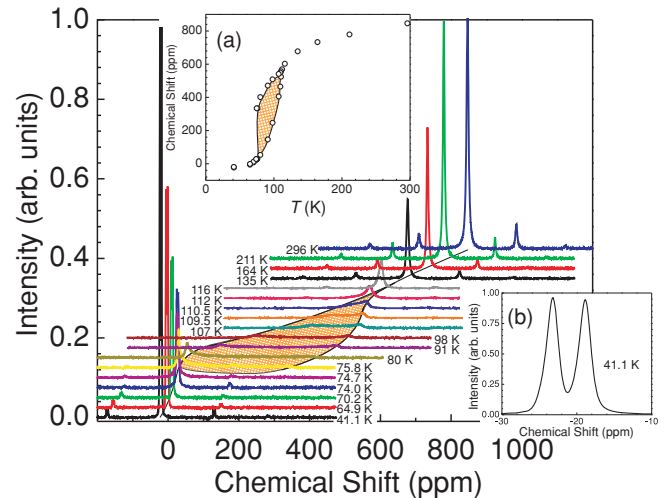
position into the interstitial position within the ribbon chains. This change is complemented by a reduction of the distance in the Ti-O-Ti NN superexchange pathway, and an increase of the intrachain O-Ti-O angle. Evidence for a structural change was not found in this temperature range, possibly due to the dynamic character of the intermediate phase as observed by nuclear magnetic resonance (NMR) (see below).

Magic angle spinning (MAS) ^{31}P NMR spectra (center field $\sim$8.5 T) operating at a spinning frequency of $\sim$25 kHz,

FIG. 2. (Color online) ^{31}P MAS NMR spectra for $TiPO_4$ (temperatures indicated). The (orange) hashed area highlights the incommensurate continuum. Insets: (a) Peak positions and/or boundary edges versus temperature. (b) The 41.1 K spectrum.
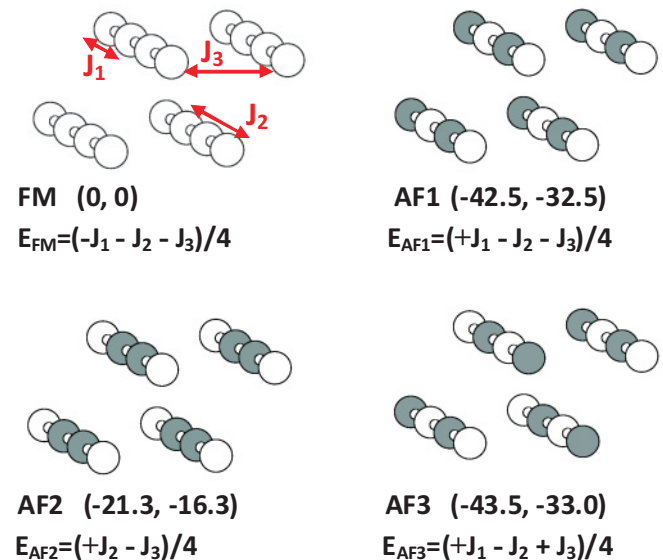

FIG. 3. (Color online) The four ordered spin configurations FM, AF1, AF2, and AF3 used to extract the values of J_1, J_2, and J_3, where only the Ti^{3+} ions are shown for simplicity. The up- and down-spin Ti^{3+} sites are indicated by different colors. The numbers in parentheses (from left to right) represent the relative energies in meV per four FUs obtained from GGA + U calculations with $U_{eff} = 2$ and 3 eV, respectively. The expression of the total SE energy per four FUs is also given.

were collected on a polycrystalline sample between $\sim$35 K and RT. The spectra are displayed versus temperature in the main panel of Fig. 2. Above $\sim$140 K we observe a single ^{31}P symmetric NMR line accompanied by two sets of very weak symmetrically placed spinning sidebands. Near 116 K the line becomes asymmetric and below 111 K it broadens into an asymmetric continuum limited by two boundary peaks. With decreasing temperature the continuum expands and its intensity decreases. Toward $\sim$76 K the continuum finally washes out, whereupon its lower boundary grows into two symmetric lines indicating the occurrence of two different P atom environments [see inset Fig. 2(b)]. The peak positions and/or boundary edges are shown versus temperature in Fig. 2(a). There are similarities between NMR measurements of $TiPO_4$, reported here, and of TiOX, reported by Saha *et al.*[26]

We now probe the SE interactions of $TiPO_4$ by performing mapping analysis based on density functional calculations.[27] We consider the NN and next-nearest-neighbor (NNN) intrachain SE interactions J_1 and J_2, respectively, as well as the interchain SE interaction J_3 (see Fig. 3). To evaluate J_1–J_3, we determine the relative energies of the four ordered spin states, FM, AF1, AF2, and AF3 shown in Fig. 3, by density functional theory (DFT) electronic band structure calculations. Our DFT calculations employed the Vienna *ab initio* simulation package[28,29] with the projected augmented-wave method, and the generalized gradient approximation (GGA) for the exchange and the correlation functional.[30] We used a plane-wave cutoff energy of 400 eV, a set of 56 **k** points in the irreducible Brillouin zone, and the threshold of 10^{-5} eV for the self-consistent-field convergence of the total electronic energy. To account for the electron correlation associated with the Ti 3d state, we performed the GGA plus on-site repulsion (GGA+U) calculations[31] with an effective $U_{eff} = U - J = 2$ and 3 eV on Ti. The relative energies, per four formula units (FUs), of the four ordered spin states are summarized in Fig. 3.

The total SE energies of the four ordered spin states can be expressed in terms of a Heisenberg spin Hamiltonian, $H = -\sum J_{ij} \vec{S}_i \vec{S}_j$, where J_{ij} is the SE interaction between the spins $\vec{S}_i$ and $\vec{S}_j$ on the spin sites i and j, respectively. By applying the energy expressions obtained for spin dimers with N unpaired spins per spin site (in the present case, $N = 1$),[32] the total SE energies for the four configurations, per four FUs, are given in Fig. 3.

Thus, by mapping the relative energies of the four ordered spin configurations given in terms of the SE parameters (see Fig. 3) onto the corresponding relative energies obtained from the GGA + U calculations, we obtained the values for the SE parameters J_1–J_3 (see Table I).[27,33] The results of our DFT calculations are in very good quantitative agreement with our experimental findings, indicating a very large NN intrachain AFM SE interaction. The NNN intrachain SE interaction is almost two orders of magnitude smaller; the interchain interaction J_3 amounts to 2% of J_1.

The low-temperature MAS data of $TiPO_4$ prove a nonmagnetic ground state with two distinct P atomic environments, as evidenced especially by the low-temperature spectra. The chemical shifts of the ^{31}P lines amount to ~-20 ppm in good agreement with what has been found for other diamagnetic orthophosphates, proving the nonmagnetic character of the

TABLE I. Values of the SE parameters J_1–J_3 derived from the mapping analysis (in K).

J_i	$U = 2$ eV	$U = 3$ eV
J_1	−988	−751
J_2	−1.4	+0.7
J_3	−20	−15

ground state of $TiPO_4$.[34,35] We ascribe the 74 K phase transition in $TiPO_4$ to a spin-Peierls transition with the Ti-Ti bond alternation within the Ti chains.

To probe the low-temperature crystal structure of $TiPO_4$, we considered the subgroups *Amm*2 and *Pmmn* of the RT space group *Cmcm*. By GGA calculations, we optimized the structures of $TiPO_4$ starting with the initial settings described by *Cmcm*, *Amm*2, and *Pmmn* without symmetry constraints in order to allow the atom positions to relax freely (with a 28 **k**-point irreducible Brillouin zone, and the thresholds of 10^{-5} eV and 0.001 eV/Å for the self-consistent-field convergence of the total electronic energy and force, respectively). The lowest-energy structure found was obtained starting from the *Pmmn* initial setting, and was lower in energy by $\sim$48 meV per formula unit than was the *Cmcm* structure, and by $\sim$32 meV per formula unit than the *Amm*2 initial structure. The structure relaxed from the *Pmmn* initial setting shows a dimerization in the Ti chains with alternating Ti-Ti distances of $\sim$2.9 and $\sim$3.5 Å, which is comparable in magnitude to that observed in TiOCl.[17] This structure also has two different environments for the P atoms within the PO_4 units, which is consistent with our MAS NMR spectra. From model calculations using the relaxed crystal structure data, we expect very weak superstructure reflections, which were not resolved in an early neutron powder diffraction experiment.[36]

The incommensurate phase seen between $\sim$111 and $\sim$74 K is similar to that found for TiOX, where it has been attributed to a frustration between the spin-Peierls pairing and an elastic interchain coupling.[20] Analogous arguments may apply for $TiPO_4$ as well. In view of the small interchain coupling the incommensurate phase between 111 and 74 K could also be ascribed to a dynamic equilibrium between short-range-ordered dimerized segments.

In conclusion, our magnetic susceptibility, heat capacity, ESR, and ^{31}P MAS NMR measurements supported by our density functional calculations show that $TiPO_4$ undergoes a spin-Peierls transition at 74.1(0.3) K, which is preceded by an incommensurate phase extending up to $\sim$111 K. The thermal hysteretic behavior of these transitions is consistent with the pattern of discontinuous and continuous transitions seen for TiOCl and TiOBr. At high temperatures the magnetic susceptibility of $TiPO_4$ is described by an $S = 1/2$ Heisenberg antiferromagnetic chain with an unprecedented NN SE of $\sim$1000 K.

*j.law@fkf.mpg.de

[1] E. Dagotto, Science **309**, 257 (2005).

[2] P. A. Lee, Rep. Prog. Phys. **71**, 012501 (2008).

[3] M. Enderle, C. Mukherjee, B. Fåk, R. K. Kremer, J.-M. Broto, H. Rosner, S.-L. Drechsler, J. Richter, J. Malek, A. Prokofiev, W. Assmus, S. Pujol, J.-L. Raggazzoni, H. Rakoto, M. Rheinstädter, and H. M. Rønnow, Europhys. Lett. **70**, 237 (2005).

[4] M. G. Banks, R. K. Kremer, C. Hoch, A. Simon, B. Ouladdiaf, J. M. Broto, H. Rakoto, C. Lee, and M.-H. Whangbo, Phys. Rev. B **80**, 024404 (2009).

[5] J. M. Law, C. Hoch, M.-H. Whangbo, and R. K. Kremer, Z. Anorg. Allg. Chem. **636**, 54 (2010).

[6] M. Isobe and Y. Ueda, J. Phys. Soc. Jpn. **65**, 1178 (1996).

[7] H. Smolinski, C. Gros, W. Weber, U. Peuchert, G. Roth, M. Weiden, and Ch. Geibel, Phys. Rev. Lett. **80**, 5164 (1998).

[8] J. Lüdecke, A. Jobst, S. van Smaalen, E. Morré, Ch. Geibel, and H.-G. Krane, Phys. Rev. Lett. **82**, 3633 (1999).

[9] M. Weiden, R. Hauptmann, C. Geibel, F. Steglich, M. Fischer, P. Lemmens, and G. Guntherodt, Z. Phys. B **103**, 1 (1997).

[10] R. J. Beynon and J. A. Wilson, J. Phys.: Condens. Matter **5**, 1983 (1993).

[11] A. Seidel, C. A. Marianetti, F. C. Chou, G. Ceder, and P. A. Lee, Phys. Rev. B **67**, 020405 (2003).

[12] V. Kataev, J. Baier, A. Moller, L. Jongen, G. Meyer, and A. Freimuth, Phys. Rev. B **68**, 140405 (2003).

[13] R. Ruckamp, J. Baier, M. Kriener, M. W. Haverkort, T. Lorenz, G. S. Uhrig, L. Jongen, A. Möller, G. Meyer, and M. Grüninger, Phys. Rev. Lett. **95**, 097203 (2005).

[14] A. Krimmel, J. Strempfer, B. Bohnenbuck, B. Keimer, M. Hoinkis, M. Klemm, S. Horn, A. Loidl, M. Sing, R. Claessen, and M. v. Zimmermann, Phys. Rev. B **73**, 172413 (2006).

[15] H. Schäfer, F. Wartenpfuhl, and E. Weise, Z. Anorg. Allg. Chem. **295**, 268 (1958).

[16] H. G. von Schnering, M. Collin, and M. Hassheider, Z. Anorg. Allg. Chem. **387**, 137 (1972).

[17] M. Shaz, S. van Smaalen, L. Palatinus, M. Hoinkis, M. Klemm, S. Horn, and R. Claessen, Phys. Rev. B **71**, 100405(R) (2005).

[18] Y.-Z. Zhang, H. O. Jeschke, and R. Valentí, Phys. Rev. B **78**, 205104 (2008).

[19] J. Hemberger, M. Hoinkis, M. Klemm, M. Sing, R. Claessen, S. Horn, and A. Loidl, Phys. Rev. B **72**, 012420 (2005).

[20] A. Schönleber, G. Shcheka, and S. van Smaalen, Phys. Rev. B **77**, 094117 (2008).

[21] J. P. Clancy, B. D. Gaulin, and F. C. Chou, Phys. Rev. B **81**, 024411 (2010).

[22] N. Kinomura and F. Muto, J. Solid State Chem. **46**, 252 (1982).

[23] R. Glaum and R. Gruehn, Z. Kristallogr. **198**, 41 (1992).

[24] D. C. Johnston, R. K. Kremer, M. Troyer, X. Wang, A. Klümper, S. L. Budko, A. F. Panchula, and P. C. Canfield, Phys. Rev. B **61**, 9558 (2000).

[25] R. Glaum and M. A. Hitchman, Austral. J. Chem. **49**, 1221 (1996).

[26] S. R. Saha, S. Golin, T. Imai, and F. C. Chou, J. Phys. Chem. Solids **68**, 2044 (2007).

[27] M.-H. Whangbo, H. J. Koo, and D. J. Dai, Solid State Chem. **176**, 417 (2003).

[28] G. Kresse and J. Hafner, Phys. Rev. B **47**, 558 (1993).

[29] G. Kresse and J. Furthmüller, Comput. Mater. Sci. **6**, 15 (1996); Phys. Rev. B **54**, 11169 (1996).

[30] J. P. Perdew, K. Burke, and M. Ernzerhof, Phys. Rev. Lett. **77**, 3865 (1996).

[31] S. L. Dudarev, G. A. Botton, S. Y. Savrasov, C. J. Humphreys, and A. P. Sutton, Phys. Rev. B **57**, 1505 (1998).

[32] D. Dai and M.-H. Whangbo, J. Chem. Phys. **114**, 2887 (2001); **118**, 29 (2003).

[33] H.-J. Koo, M.-H. Whangbo, and K.-S. Lee, Inorg. Chem. **42**, 5932 (2003).

[34] A. K. Cheetham, N. J. Clayden, C. M. Dobson, and R. J. B. Jakeman, J. Chem. Soc., Chem. Commun. **1986**, 195.

[35] G. L. Turner, K. A. Smith, R. J. Kirkpatrick, and E. Oldfield, J. Magn. Reson. **67**, 544 (1986).

[36] R. Glaum, M. Reehuis, N. Stüßer, U. Kaiser, and F. Reinauer, J. Solid State Chem. **126**, 15 (1996).